AlfaMC: A fast alpha particle transport Monte Carlo code

Luis Peralta [a,b,*], Alina Louro [b]

[a] Faculdade de Ciências da Universidade de Lisboa, Portugal
[b] Laboratório de Instrumentação e Física Experimental de Partículas, Portugal

ARTICLE INFO

ABSTRACT

AlfaMC is a Monte Carlo simulation code for the transport of alpha particles. This code is based on the Continuous Slowing Down Approximation and uses the NIST/ASTAR stopping-power database. The code uses a powerful geometrical package, which allows coding of complex geometries. A flexible histogramming package is used as well, which greatly eases the scoring of results. The code is tailored for microdosimetric applications in which speed is a key factor. Comparison with the SRIM code is made for deposited energy in thin layers and range for air, mylar, aluminum and gold. The general agreement between the two codes is good for beam energies between 1 and 12 MeV.

© 2013 Elsevier B.V. All rights reserved.

1. Introduction

Alpha particles are highly ionizing and have low penetration in matter. Their energy ranges from 1.830 MeV (^{144}Nd) to 11.740 MeV (^{266m}Mt) [1], although most common alpha sources will emit particles in the 4–9 MeV range [1]. In condensed matter their range is typically below 100 μm, while in air at STP they can reach a few centimeters [2,3]. The energy transfer from an alpha particle to an atomic electron in a single collision is small. For non-relativistic particles of relative velocity β and $\gamma = 1/\sqrt{1-\beta^2}$ the maximum energy transfer T_{max} to an electron of mass m_e is approximately given by [3] $T_{max} \approx 2m_e c^2 \beta^2 \gamma^2$, where c is the speed of light. For an alpha particle of 10 MeV this results in a maximum energy transfer of only 5.4 keV. For liquid water an electron with energy below 10 keV has a range inferior to 2.5 μm [2]. These electrons will lose their energy in the vicinity of the interaction point with the alpha particle and their transport can be neglected by the Monte Carlo code. Due to the alpha particle's high mass, the emission of bremsstrahlung radiation at these energies is completely negligible. For these reasons the Continuous Slowing Down Approximation (CSDA) [3] which assumes that a charged particle loses energy continuously along its path at the linear rate given by the instantaneous stopping power is an adequate approximation at this energy range.

General-purpose Monte Carlo programs as MCNPX, GEANT3, GEANT4 or FLUKA [4–8] can simulate the transport and energy loss of alpha particles in matter. They can simulate complex geometries, but they are not optimized for speed. Depending on the primary particle energy, applied cuts, number of requested events, etc., a simulation can take between a few minutes to a considerable number of hours. Due to their complexity, the learning curve of the novice user has in general a moderate slope and several days might be needed to obtain a meaningful result. The state-of-the-art SRIM program [9,10], for ion tracking in matter, on the other hand has a straightforward implementation, but allows only a simple slab geometry.

Thus, there is need for a fast Monte Carlo package capable of dealing with complex geometries, easy to implement and that can give meaningful results in a few minutes. The AlfaMC package was initially developed in the framework of cell irradiation by alpha particles where the program's results are expected to be accurate for cell sizes bigger than 10 μm. The program is used within our group to simulate the interaction of alpha particles with cells of the respiratory tree [11]. Other applications of the program are the study of cancer therapy with alpha particles, environmental studies involving alpha particles or fast computation of alpha particle energy loss in thin layers.

2. AlfaMC physical model

The package is able to simulate complex geometrical bodies and spatially-distributed alpha particle sources. It has a sophisticated scoring and histogramming set of routines. The package uses the National Institute of Standards and Technology (NIST) ASTAR database where stopping powers for 74 materials, 26 elements and 48 compounds and mixtures, are available. Stopping power data for new materials based on this set can be generated using the Alfamaterial.f program included in the package. The alpha particle

* Corresponding author. Tel.: +351 217500945.
E-mail address: luis@lip.pt (L. Peralta).

transport is based on the Continuous Slowing Down Approximation. Gaussian or Landau distributed energy straggling is performed. A simple Fermi small-angle multiple scattering model is adopted. The adopted physical model is a valid approximation in the 1–12 MeV energy range.

2.1. Stopping-power computation

Alpha particles interact with the electrons and nuclei of the medium, primarily through the Coulomb electric force. Most of these interactions are in fact with the atomic electrons and individually transfer only minute fractions of the incident particle's kinetic energy. It is a convenient approximation to regard the alpha particle as losing its kinetic energy gradually and without hard collisions with atomic electrons in a process referred to as "Continuous Slowing-Down Approximation".

Based on the CSDA the AlfaMC code assumes that the average energy loss per unit length is given by the unrestricted stopping power of the alpha particle. The NIST ASTAR database [2] supplies separate values for the electronic and nuclear stopping power, while AlfaMC adds both values to obtain the total stopping power value. Original ASTAR tables present stopping power values for 122 energy values between 0.001 MeV and 1000 MeV, distributed on a logarithmic grid. The AlfaMC code then computes stopping power values S' on a linear energy grid of 0.001 MeV in energy range of 0.001–100 MeV. To obtain the interpolated S values, a logarithmic interpolation of the ASTAR stopping power S values is made.

For unevenly spaced grids and non-linear functions the logarithmic interpolation will give a better approximation to the function value than one that can be obtained with a linear interpolation. The use of pre-computed lookup tables greatly improves the computation time, since computation of stopping powers is one of the most frequently performed operations.

2.2. Energy straggling

The energy loss of an alpha particle is a stochastic quantity with a distribution often called straggling function. In the tracking model adopted by AlfaMC, no secondary particles are produced and continuous energy loss is unrestricted. For thick slabs, the energy loss distribution approaches a Gaussian [12], but for thin traversed slabs other distributions can be considered [6,12,13]. A cut parameter κ can be defined to set the limit between the thin and thick slab as [6,12] $\Delta E = \kappa T_{max}$ where ΔE is the energy deposited in the slab and T_{max} the maximum energy transfer in a single collision given by [14]

$$T_{max} = \frac{2m_e c^2 \beta^2 \gamma^2}{1 + 2\gamma m_e/m_\alpha + m_e^2/m_\alpha^2} \quad (1)$$

where m_α is the alpha particle mass.

Usually it is assumed that for $\kappa > 10$ the Gaussian model is a good approximation, while for the intermediate values $0.01 \leq \kappa < 10$ the straggling function follows a Vavilov [15,16] distribution. For lower κ values (i.e. $\kappa \leq 0.01$), the energy straggling function is given by the Landau distribution [17,12].

The AlfaMC code has two options on what concerns energy straggling. The default option uses only the Gaussian model. A second option uses the Gaussian/Vavilov/Landau models depending on the κ parameter. This option is slower than the former one. In most cases the difference introduced in the energy FWHM is small so the option to use only the Gaussian model is a reasonable one. The routines needed to generate the Vavilov and Landau distributions are not native to AlfaMC and are supplied in a separate library.

2.2.1. The Gaussian distribution

If the number of collisions of the alpha particle with atomic electrons when traversing an absorber is large and energy losses can be considered as independent, then the Central Limit Theorem can be applied. A Gaussian distribution is then expected for the energy loss in the absorber with a certain standard deviation. Several forms have been proposed for this Gaussian straggling distribution. The first form was proposed by Niels Bohr in 1913 [18]. In his model, the variance of energy loss distribution was given as [19–21]

$$\sigma_B^2 = 4\pi \left(\frac{e^2}{4\pi\varepsilon_0}\right)^2 z_\alpha^2 Z N \Delta x \quad (2)$$

where e is the elementary charge, ε_0 the vacuum permittivity, N the number of atoms per unit volume, Δx the slab thickness, Z the medium atomic number and z_α the alpha particle atomic number. Since $N = \rho N_A/A$ where ρ is the density, A the atomic weight and N_A the Avogadro number, using the relation $r_e = (1/4\pi\varepsilon_0)e^2/m_e c^2$ the variance can be written as

$$\sigma_B^2 = 4\pi r_e^2 (m_e c^2)^2 z_\alpha^2 \frac{Z}{A} \rho N_A \Delta x \quad (3)$$

with Δx in cm and ρ in g/cm³.

A quantum mechanical theory has been developed by Bethe and Livingston [13,20,22] who found a value for the variance equal to

$$\sigma_{BL}^2 = 4\pi \left(\frac{e^2}{4\pi\varepsilon_0}\right)^2 z_\alpha^2 N\left(Z' + \sum_i \frac{8}{3}\left(\frac{I_i Z_i}{T_{max}}\right)\ln\left(\frac{T_{max}}{I_i}\right)\right)\Delta x \quad (4)$$

where Z' is the effective atomic number [20], I_i and Z_i are the ionization potential and number of electrons of i shell of the stopping atom. While Bohr's result is independent of the particle energy, the Bethe-Linvingston's result has a small energy dependence, relevant for high energies [13].

More comprehensive theories have been developed for thick slabs such as Payne [23] or Tschalar theories [24] but from the Monte Carlo point of view these theories have a more complex implementation and are not suitable for a fast Monte Carlo code. The GEANT3 and GEANT4 MC codes [6,25] use an alternative formulation for Gaussian variance which is based on the work of Seltzer and Berger [16,26] suitable for a fast Monte Carlo program and adopted by AlfaMC. This formulation introduces a correction to the energy straggling variance depending on the particle's relative velocity β and maximum energy transfer T_{max}

$$\sigma^2 = \frac{2\pi r_e^2 mc^2 z_\alpha^2 Z\rho N_A \Delta x}{\beta^2 A} T_{max}\left(1 - \frac{\beta^2}{2}\right). \quad (5)$$

For alpha particles the correction introduced by this formula relative to σ_B is small. In fact since the maximum energy transfer in a single collision is given by Eq. 1 in the limit $m_e \ll m_\alpha$ and $\gamma \approx 1$ we get $T_{max} \approx 2m_e c^2 \beta^2 = 1.022\beta^2$ MeV. Under these conditions, the relative velocity is much less than the unit so that $(1 - \beta^2/2) \approx 1$ and finally $\sigma^2 \approx \sigma_B^2$.

2.2.2. The Landau distribution

For very thin absorbers or gases the number of collisions can be too small for the Central Limit Theorem to hold. Large energy fluctuations are possible and the straggling function is no longer symmetrical. If the mean energy loss is approximated by Bethe–Bloch non-logarithmic factor

$$\overline{E_{loss}} = \xi = \frac{2\pi r_e^2 mc^2 z_\alpha^2 Z\rho N_A \Delta x}{\beta^2 A} \quad (6)$$

the cut parameter will be given by $\kappa = \xi/T_{max}$. For $\kappa \leq 0.01$ the straggling distribution is successfully described by Landau theory

[17]. For energy loss ε the Landau distribution $f(\varepsilon, \Delta x)$ may be written in terms of a universal $\phi(\lambda)$ function such as

$$f(\varepsilon, \Delta x) = = \frac{1}{\xi}\phi(\lambda). \tag{7}$$

The Landau variable λ is defined as [6]

$$\lambda = \frac{\varepsilon - \overline{E_{loss}}}{\xi} - (1 - C) - \beta^2 - \ln\left(\frac{\xi}{T_{max}}\right) \tag{8}$$

where $C = 0.577215...$ is Euler's constant. To generate $\phi(\lambda)$, AlfaMC uses a modified version of the routine GLANDG [6] from GEANT3.

2.2.3. The Vavilov distribution

For intermediate thickness absorbers where $0.01 \leq \kappa < 10$ energy loss distribution can be obtained from Vavilov theory [15,16]. This theory relates energy loss distribution $f(\varepsilon, \Delta x)$ of a charged particle with a universal function $\phi_v(\lambda_v, \kappa, \beta^2)$ in just the same way as the Landau theory

$$f(\varepsilon, \Delta x) = \frac{1}{\xi}\phi(\lambda_v, \kappa, \beta^2) \tag{9}$$

where the Vavilov variable λ_v is defined as [6]

$$\lambda_v = \kappa\left(\frac{\varepsilon - \overline{E_{loss}}}{\xi} - (1 - C) - \beta^2\right). \tag{10}$$

The Vavilov λ_v is related to λ by the relation [6] $\lambda = \lambda_v/\kappa - \ln(\kappa)$ and the relation between λ and the energy loss is

$$\lambda_v/\kappa = \lambda + \ln(\kappa) = \left(\frac{\varepsilon - \overline{E_{loss}}}{\xi} - (1 - C) - \beta^2\right). \tag{11}$$

AlfaMC uses GVAVIV routine from GEANT3 that samples λ Landau instead of λ_v variable.

2.3. Alpha particle multiple scattering

An alpha particle traversing a medium is deflected through many small angles, mostly due to Coulomb scattering from nuclei. The distribution of the scattering angle after traversing a small layer is roughly Gaussian for small angle values. For large angles the distribution has a Rutherford scattering-like behavior, with larger tails than those of a Gaussian distribution. Molière's [27] and Fermi's [28] theories have been widely used to describe the multiple scattering of heavy charged particles. The theory of Fermi results in the Gaussian approximation for small angles has an intuitive physical meaning and is easy to implement in the MC code. For these reasons it was adopted as the multiple scattering model in AlfaMC.

For a particle traversing a thin slab of matter of thickness s with incidence direction along the z axis, one can define the deflection angles θ_x and θ_y, measured relatively to the incidence direction in the xz and yz planes (Fig. 1). According to Fermi's theory [14,29] θ_x and θ_y deflection angles have independent Gaussian distributions given by
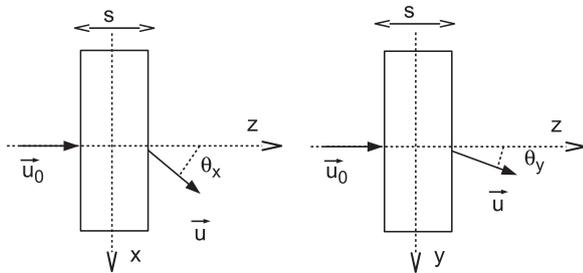
$$\frac{dN}{d\theta_i} = \frac{1}{\sqrt{2\pi}\theta_0}\exp\left(-\frac{\theta_i^2}{2\theta_0^2}\right) \tag{12}$$

with $i = x, y$.

Standard deviation of the distribution θ_0 can be approximated by [14,29]

$$\theta_0 = \frac{13.6\,\text{MeV}}{pc\beta}Z_\alpha\sqrt{\frac{s}{X_0}} \tag{13}$$

where X_0 is the material radiation length. Lynch and Dahl [30] have looked into the problem of parameterizing θ_0 and propose several other approximations. The formula adopted by AlfaMC was

$$\theta_0 = \frac{4}{5} \times \frac{13.6\,\text{MeV}}{pc\beta}Z_\alpha\sqrt{\frac{s}{X_0}}\left[1 + 0.038\ln\left(\frac{sZ_\alpha^2}{X_0\beta^2}\right)\right] \tag{14}$$

where the 4/5 factor was empirically determined, for better comparison with the SRIM results (see Section 5).

The material radiation length X_0 has been calculated and tabulated by Tsai [14,31]. Eqs. (13) and (14) are applicable to the full path of length s. Dividing this path into steps (i.e. $s = s_1 + s_2$) will introduce a bias since $\theta_0(s_1 + s_2) \neq \sqrt{\theta_0^2(s_1) + \theta_0^2(s_2)}$. AlfaMC neglects this effect, introducing a systematic bias in the lateral straggling.

In Monte Carlo transport of an alpha particle due to multiple scattering, the actual path length t made by the alpha particle is bigger than step s (Fig. 2). From the Fermi–Eyges theory we have the relation [32]

$$t = s + \frac{1}{2}\int_0^t \theta_0^2(t')dt' \tag{15}$$

where $\theta_0(t)$ is given by Eq. 13. Assuming a constant momentum p during the step and approximating t by s in the integral one gets:

$$t \approx s + \frac{K}{4}s^2 \tag{16}$$

where $K = [(13.6\,\text{MeV})Z_\alpha/pc\beta]^2/X_0$ and X_0 is in cm. For 1 μm steps or smaller the correction is less than 0.1% for low Z materials and energies above 1 MeV. The correction becomes more important as the alpha particle decreases energy and $\theta_0(t)$ increases. The correction could also be important for high-Z materials where $\theta_0(t)$ also has a larger value due to the increase in the Coulomb cross-section.

Apart from the path length correction, there is also a transverse correction. In fact the particle position after a step s is computed as $(x', y, z) = (x_0, y_0, z_0) + s\,\overrightarrow{u_0}$ where $\overrightarrow{u_0} = (u_0, v_0, w_0)$ is the particle's direction vector entering the slab. Due to multiple scattering the particle position should be (x', y', z'), a distance ρ from (x, y, z). Since t is bigger than the triangle hypotenuse we can say that $\rho^2 < t^2 - s^2 \approx (s + K/4s^2)^2 - s^2 = K/2s^3 + (K/4)^2s^4$. As far as s stays small and $t \approx s$ the lateral displacement ρ is very small and can be neglected.

3. The program flow

The AlfaMC code is written in Fortran language and the main code is found in the library AlfaMCLIB.f. It uses the ULYSSES [33]
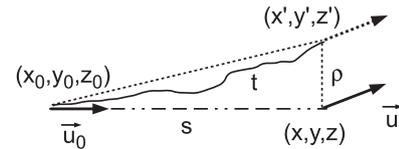

Fig. 1. Definition of the θ_x and θ_y deflection angles.

Fig. 2. Relation between particle's step s and the actual path length t.

package for the particle tracking in the geometry and ULHISTOS package for scoring and histogramming [34]. ULYSSES is a package, designed to make particle tracking in complex volumes and score the results. The histogramming routines are grouped in a library called ULHISTOS. The ULYSSES package is also written in FORTRAN. There are several volumes available in ULYSSES that can be used to build complex bodies. Examples of available volumes are the rectangular box, the cylinder, the sphere, the cone, etc. Volumes can be rotated in space. The geometry system used by ULYSSES allows for the construction of rather complex structures by adding (or subtracting) volumes. The volume organization is made using mother–daughter logic. Any volume may have daughter volumes inside. All the volumes have a mother volume except the universe volume which contains all volumes. A volume may have more than one mother, that is, it may be shared by more than one volume. The scoring of results is handled by the ULHISTOS library. One or two-dimensional histograms are possible. Apart from booking, filling and outputting histograms, the ULHISTOS library contains several routines to perform operations on histograms and to extract statistical results.

The code is driven by a main routine which controls the program flow. A routine containing the geometry description must be supplied by the user. This routine (ulgeom.f) must use ULYSSES package routines to build the geometrical setup. A radiation source routine containing the code for the generation of the alpha particle initial parameters (e.g. position, direction and energy) must also be supplied by the user. Examples of such routines are available with the AlfaMC package distribution.

The flowchart of the main routine is presented in Fig. 3. The program starts by initializing general parameters in the ULYSSES and ULHISTOS databases. Parameters like the number of events to be generated, number of materials and general cuts (energy and step size) are also set. The necessary histograms are then booked. The data files containing stopping power tables and other data characterizing the material media are also read. Then the routine ulgeom.f containing the geometrical description of the setup is called. After that the program enters the main event loop where each alpha particle is generated and tracked through the geometry. Generation of alpha particle initial properties (position, direction and kinetic energy) is made in routine ulsource.f that must be supplied by the user. The program then finds the volume inside which the particle is generated. A step size is then computed according to the percentage of energy loss allowed for each step, which is set by the user. This variable must have a value between 0 and 1. The next step size s is computed according to the particle stopping power and energy loss in the step. If the computed value is lower or higher than the step size cuts defined by the user, step size reverts to the limit. The particle is then tracked through the geometry.

Results such as beam fluencies or deposited energy in the tracking volume can be scored. After this step the program checks if the particle still has energy above the energy cut and did not exit the setup. If both requirements are met, the program will advance the particle one more step. If not, then event final results (like the total deposited energy in a volume) are scored, and the program will generate a new particle. When the total number of requested particles is generated the program outputs the final results. Fig. 4 shows an example of 0.5 MeV alpha particle tracks in air simulated with AlfaMC.

4. The materials database

The AlfaMC package provides the program AlfaMaterial.f to compute stopping-power data. The program uses data from the NIST/ASTAR [2] database for computation of stopping-power.
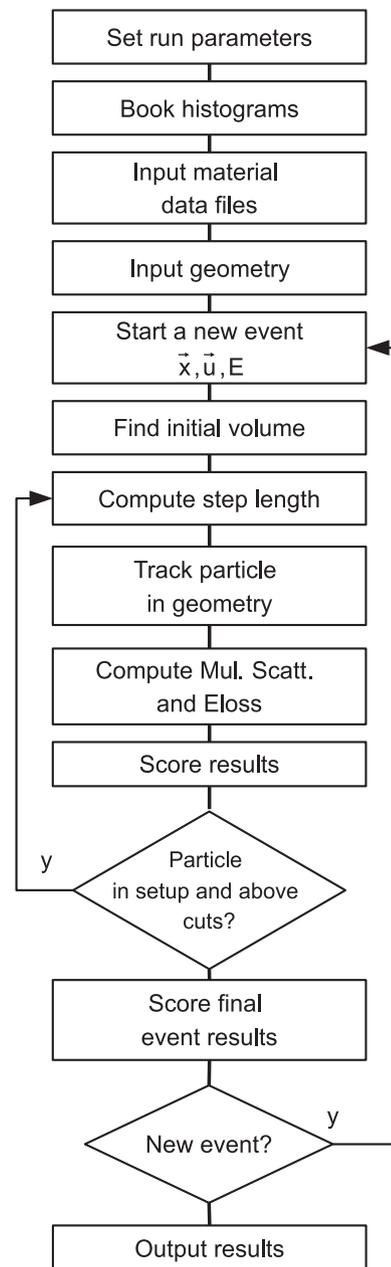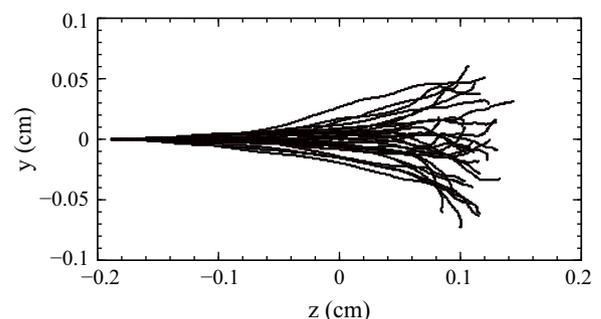
Fig. 3. The program flowchart.

Fig. 4. Simulation of a 0.5 MeV alpha particle beam in air.

The ASTAR program calculates stopping-power and range tables for helium ions in 74 materials, according to methods described in ICRU Report 49 [35] and is briefly explained in the NIST/ASTAR website [36]. This list includes 26 elements and 48 compounds

and mixtures. The available energy ranges between 0.001 and 1000 MeV. AlfaMC package provides data files with the electronic and nuclear stopping-powers and ranges. For compounds and mixtures an additional file containing the material composition is also provided. The AlfaMaterial program computes the stopping-power of user-defined materials using the Bragg rule [35,37]:

$$\frac{1}{\rho}\frac{dE}{dx} = \sum_i \frac{w_i}{\rho_i}\left(\frac{dE}{dx}\right)_i \qquad (17)$$

where w_i and ρ_i are the fraction by weight and density of the ith element.

Besides stopping-power, AlfaMaterial also computes other useful parameters for the tracking of alpha particles, namely the radiation length X_0, the mean excitation energy, the effective atomic number and effective mass number. The radiation length of compounds or mixtures is approximated by

$$\frac{1}{X_0} = \sum_j \frac{w_j}{X_{0j}} \qquad (18)$$

where X_{0j} is the radiation length of the jth element.

The mean excitation energy value I for elements is obtained from the table available at NIST [37]. For a compound or mixture, the mean excitation energy value can be approximated by [38,39]

$$\ln(I) = \frac{\sum w_i(Z_i/A_i)\ln(I_i)}{\sum w_i(Z_i/A_i)} \qquad (19)$$

where w_i is the proportion by weight of element i. In the case of a compound

$$w_i = \frac{N_i A_i}{\sum N_i A_i} \qquad (20)$$

where N_i is the number of atoms of element i in the compound. The atomic weights of elements are obtained from [40,41].

5. Comparison with SRIM

The SRIM program [9] contains updated values of the stopping powers for most ion nuclei including helium ions. Using a simple slab geometry, several physical quantities can be compared when computed by AlphaMC and SRIM. The comparison will be made for 4 different types of media: a gas (air) 3 mm thick, a low Z medium with absorption properties close to human tissue (mylar) 3 μm thick, a medium Z absorbent material (aluminum) 2 μm thick and a high-Z material (gold) 1 μm thick. Thicknesses where chosen in such a way that, percentage energy loss is of same order of magnitude for all 4 targets. For each data point a run of 10000 events was made.

5.1. Deposited energy

The deposited energy of alpha particles traversing different thicknesses of the four chosen media is computed by AlfaMC and SRIM program. Beam energy ranges from 1–12 MeV. The average value and standard deviation (energy dispersion) were computed using a 3σ interval. This procedure minimizes the bias due to non-Gaussian tails.

For energy beams greater than 2 MeV, the agreement between the deposited energy computed by SRIM and AlfaMC (Fig. 5) is within 5% and better 6% for energies above 1 MeV. On what concerns the energy dispersion due to straggling (Fig. 6), the general agreement between the energy standard deviation of SRIM and AlfaMC is within 6% for energy values greater than 2 MeV.
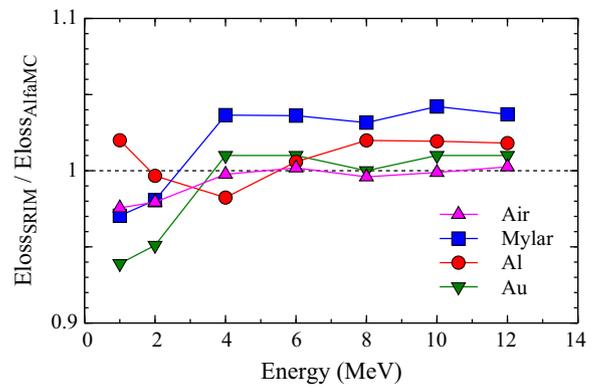

Fig. 5. SRIM/AlfaMC ratio of alpha particle deposited energy for layers of air, mylar, aluminum and gold. Uncertainties are within 1%.
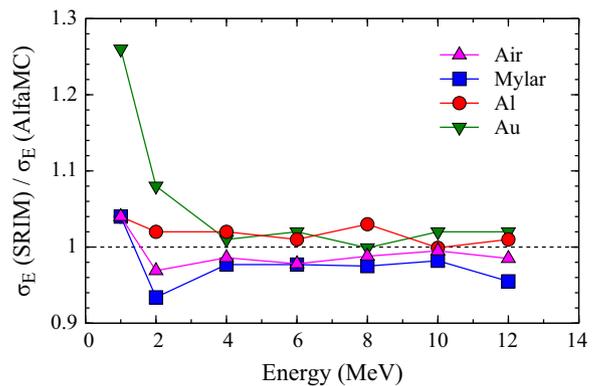

Fig. 6. SRIM/AlfaMC ratio of alpha particle energy dispersion for layers of air, mylar, aluminum and gold. Uncertainties are within 2%.
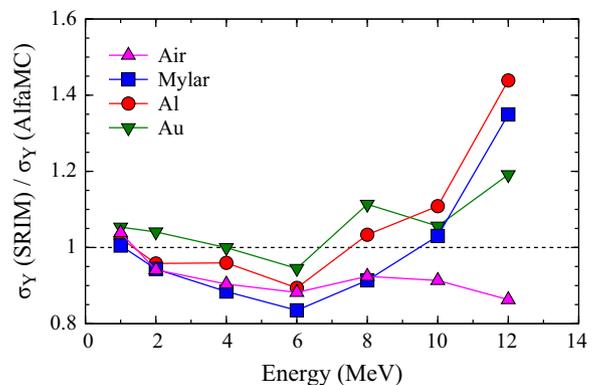

Fig. 7. The SRIM/AlfaMC ratio for lateral straggling in air (3 mm), mylar (3 mm), aluminum (2 μm) and gold (1 μm) in the 1–12 MeV range. Uncertainties are within 1%.

5.2. Lateral dispersion

The value of the lateral dispersion on the coordinates perpendicular to the beam axis (standard deviation on x or y distribution) is a measure of the multiple scattering lateral straggling. For air, mylar, aluminum and gold the value of the lateral dispersion has been computed by AlfaMC and compared to the value obtained in the SRIM simulation in the 1–12 MeV range. Obtained results are presented in Fig. 7.

We conclude that the model gives a satisfactory description of multiple scattering lateral straggling for the studied range. The deviation of AlfaMC from SRIM is between 10% and 20% for energy values up to 10 MeV.
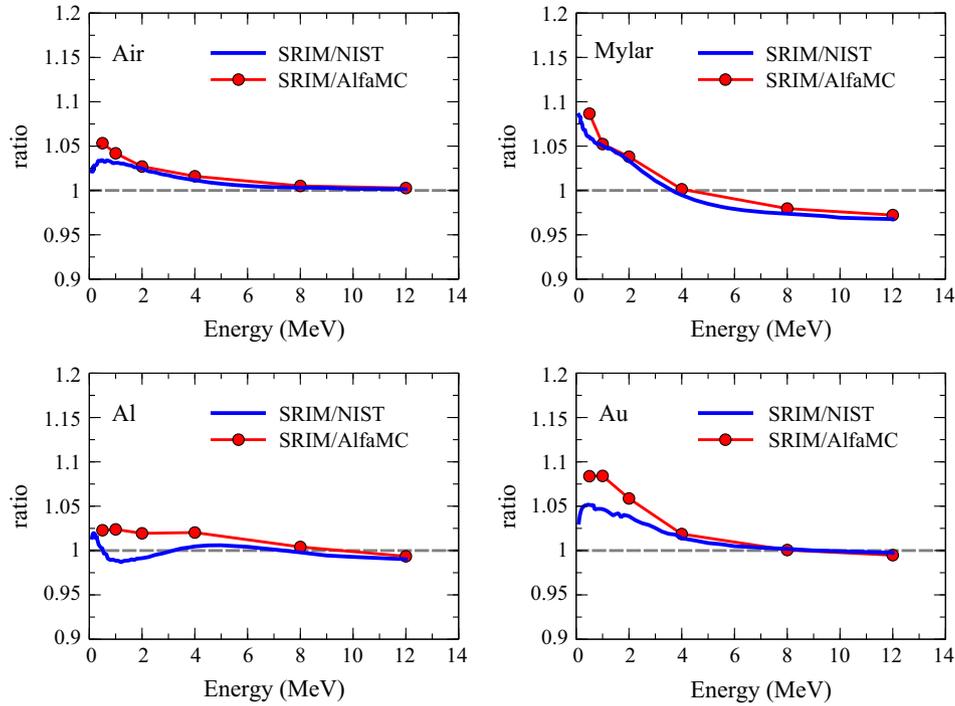
Fig. 8. Projected range ratios between SRIM and AlfaMC for air, mylar aluminum and gold. The continuous line is the SRIM/NIST ratio for projected range. Uncertainties are within 1%.
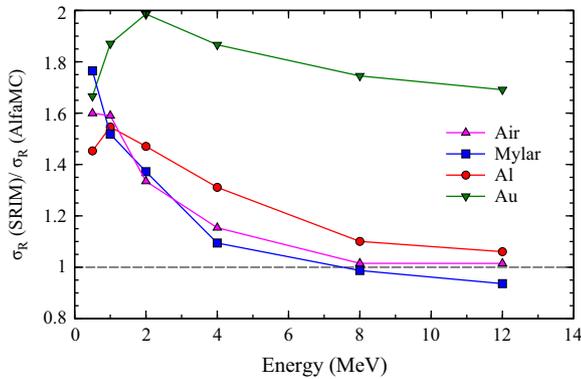

Fig. 9. Range straggling parameter ratios between SRIM and AlfaMC for air, mylar, aluminum and gold. Uncertainties are within 1%.

5.3. Range of alpha particles

The *CSDA range* [38] representing the pathlength of the particle in the CSDA approximation can be computed from the stopping power by

$$R_{CSDA} = \int_0^{T_0} \left(\frac{dE}{dx}\right)^{-1} dE \qquad (21)$$

where T_0 is the particle's initial kinetic energy. Another closely related quantity is the *projected range*. As defined by Attix [38] "the projected range $\langle t \rangle$ of a charged particle of a given type and initial energy in a given medium is the expectation value of the farthest depth of penetration of the particle in its initial direction". This is a quantity that can be experimentally determined in a transmission experiment. We can think of a pencil beam of particles perpendicularly traversing a variable thickness slab and measuring the number of particles that come out of the slab as we increase the slab thickness. For heavy charged particles, excluding cases of nuclear interaction, almost all of them will transverse the absorbing material until a certain thickness t_1 is reached. After that thickness a rapid decrease on the detected number of particles is observed. The thickness t_{max} for which no charged particle comes out of the slab is called the *maximum penetration depth*. The projected range can be obtained as

$$\langle t \rangle = \int_{t_1}^{t_{max}} t\frac{dN(t)}{dt} dt \Big/ \int_{t_1}^{t_{max}} \frac{dN(t)}{dt} dt \qquad (22)$$

where $dN(t)/dt$ is the number of particles stopping at depths between t and $t+dt$.

All of these quantities can be obtained by simulation. The *CSDA range* is obtained as the average over the number of simulated alpha particles of the sum of all steps given during the transport of each alpha particle. This program uses the multiple scattering corrected step to obtain the value of the *CSDA range*. P*rojected range* is obtained by AlfaMC as the average depth of penetration of the alpha particles up to their full stop.

The *projected range* was computed by AlfaMC and SRIM for air, mylar, aluminum and gold for a number of energies in the range 0.5–12 MeV. Fig. 8 shows the ratio of the *projected range* as computed by SRIM and AlfaMC as a function of the particle's kinetic energy. The ratio of the *projected range* given by SRIM and NIST in their original tables is also presented.

We start noticing differences between projected ranges given by SRIM and NIST/ASTAR tables for low energies, which can be as much as 9%. On what concerns AlfaMC, from these results we conclude that for alpha energies above 0.5 MeV the computed SRIM/AlfaMC range ratios agree with SRIM/NIST range ratio within 2–3% at energies up to 2 MeV and is better than that for higher energies.

Range straggling is a parameter where SRIM and AlfaMC show considerable differences. Fig. 9 presents the range standard deviation ratios between SRIM and AlfaMC. It can be seen that, with the exception of high energy values, the range straggling in SRIM has larger values than in AlfaMC. This can in part be due to the non-Gaussian, high angle multiple scattering which is not present in AlfaMC.
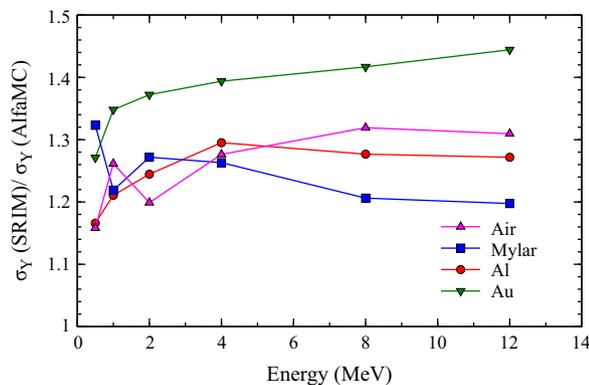
Fig. 10. Lateral straggling parameter ratios between SRIM and AlfaMC for air, mylar, aluminum and gold. Uncertainties are within 1%.

This difference in the multiple scattering models is particularly important at the end of the alpha particle path where their energy is low. As expected, the lateral dispersion at the end of the path has larger values for SRIM. This can be confirmed in Fig. 10 where the ratios between the standard deviations of the lateral dispersion curves are presented for air, mylar, aluminum and gold.

6. Discussion and conclusions

AlfaMC is a fast MC for the transport of alpha particles in complex geometries. The program uses the ASTAR/NIST precomputed stopping power tables to get the alpha particles energy loss. The default energy straggling is assumed to be Gaussian, but a more comprehensive description using the Vavilov and Landau distributions is also available using modified routines from GEANT3. A simple model is adopted for the multiple Coulomb scattering, based on a Gaussian distribution. The need to use a fast, multiple scattering sampling distributions is a major cause for uncertainty in AlfaMC at low energies.

When slowing down in matter ions will capture electrons from the medium reducing the effective electrical charge. The effect is somehow taken into account in the NIST/ASTAR stopping-power values since in the low-energy region they are calculated from fitting formulas that represent experimental data for many elements and a limited number of compounds [36]. The effect is not taken into account in the computation of the energy straggling or multiple scattering, since a reduction in the effective charge from $+2e$ would decrease both effects at low energy, increasing the difference to SRIM results.

The comparison with the well established SRIM program shows that AlfaMC can deliver meaningful results in the 1–12 MeV range for the alpha particle's energy. For energies lower than 1 MeV, differences greater than 10% can be found between the results of both programs.

The AlfaMC program speed was compared with SRIM and the general-purpose Monte Carlo code FLUKA running on the same CPU for a simple slab geometry. A 10 MeV alpha particle beam was set to irradiate a 10 μm-thick Al foil. Under these conditions the particle losses about 1 MeV crossing the foil and eventual different cut-offs have little influence in program speed. This is important since SRIM does not allow any user cut-off control. It was found that, per event, the ratio of spent time between FLUKA and AlfaMC was 5, while the ratio of spent time between SRIM and AlfaMC was 63.

The AlfaMC code, as well as the ULYSSES and ULHISTOS packages are open-source codes released under the General Public Licence (GPL) and can be obtained from the site http://www.lip.pt/alfamc.

References

[1] R.B. Firestone, L.P. Ekström, Table of Radioactive Isotopes, Electronic edition, 2004, ⟨http://ie.lbl.gov/toi/⟩ (accessed 2012).
[2] M.J. Berger, J.S. Coursey, M.A. Zucker, J. Chang, Stopping-power and range tables for helium ions, 2011, ⟨http://physics.nist.gov/PhysRefData/Star/Text/ASTAR.html⟩ (accessed 2012).
[3] J.E. Turner, Atoms, Radiation, and Radiation Protection, Wiley-VCH, Weinheim, 2007.
[4] S. Agostinelli, et al., Nucl. Instrum. Methods Phys. Res. Sect. A: Accel. Spectrom. Detect. Assoc. Equip. 506 (3) (2003) 250.
[5] J. Allison, et al., IEEE Trans. Nucl. Sci. 53 (1) (2006) 270.
[6] GEANT, CERN Program Library Long Writeup W5013, GEANT Detector Description and simulation tool, 1993, ⟨http://wwwinfo.cern.ch/asdoc/pdfdir/geant.pdf⟩ (accessed 2012).
[7] MCNPX, 2011, ⟨http://mcnpx.lanl.gov⟩ (accessed 2012).
[8] FLUKA, 2010, ⟨http://www.fluka.org⟩ (accessed 2012).
[9] SRIM, 2008, ⟨http://www.srim.org/⟩ (accessed 2012).
[10] J.F. Ziegler, J.P. Biersack, The Stopping and Range of Ions in Solids, Pergamon Press, New York, 1985.
[11] A. Louro, Da temática do radão na região da Guarda à construção de um modelo microdosimétrico. O caso particular do acino pulmunar humano (Ph.D. thesis), Universidade da Beira Interior, Portugal, 2013 (in portuguese).
[12] W.R. Leo, Techniques for Nuclear and Particle Physics Experiments: A How-To Approach, Springer, Berlin, 1994.
[13] N. Tsoulfanidis, Measurement and Detection of Radiation, Taylor & Francis, Washington, DC, 1995.
[14] J. Beringer, et al., (Particle Data Group), Phys. Rev. D86 (2012) 010001. (accessed 2012)http://pdg.lbl.gov/.
[15] P.V. Vavilov, Sov. Phys. JETP 5 (1957) 749.
[16] B. Schorr, Comput. Phys. Commun. 7 (1974) 216.
[17] L.D. Landau, J. Phys. USSR 8 (1944) 201.
[18] N. Bohr, Philos. Mag. 25 (1913) 10.
[19] J.J. Ramirez, R.M. Prior, J.B. Swint, A.R. Quinton, R.A. Blue, Phys. Rev. 179 (1969) 310.
[20] R.B. Strittmatter, B.W. Wehring, Nucl. Instrum. Methods 135 (1976) 173.
[21] W.R. Chu, Phys. Rev. A 13 (1976) 2057.
[22] M.S. Livingston, H. Bethe, Rev. Mod. Phys. 9 (1937) 245.
[23] M.G. Payne, Phys. Rev. 185 (1969) 611.
[24] C. Tschalar, H.D. Maccabee, Phys. Rev. B 1 (1970) 2863.
[25] GEANT4, 2011, ⟨http://geant4.web.cern.ch/geant4/UserDocumentation/Users Guides/PhysicsReferenceManual/fo/PhysicsReferenceManual.pdf⟩ (accessed 2012).
[26] S.M. Seltzer, M.J. Berger, Energy loss straggling of protons and mesons. In studies in penetration of charged particles in matter. Nuclear Science Series 39, National Academy of Sciences, Washington DC, 1964.
[27] H.A. Bethe, Phys. Rev. 89 (1953) 1256.
[28] B. Rossi, K. Greisen, Rev. Mod. Phys. 13 (1941) 240.
[29] M. Wong, W. Schimmerling, M.H. Phillips, B.A. Ludewigt, D.A. Landis, J.T. Walton, S.B. Curtis, Med. Phys. 17 (1990) 163.
[30] G.R. Lynch, O.I. Dahl, Nucl. Instrum. Methods B58 (1991) 6.
[31] Y.S. Tsai, Rev. Mod. Phys. 46 (1974) 815.
[32] W.R. Nelson, et al., The EGS4 code system, Technical Report 265, SLAC, 1985.
[33] Ulysses, 2012, ⟨http://www.lip.pt/ulysses/Ulysses_manual.pdf⟩ (accessed 2012).
[34] Ulhistos, 2012, ⟨http://www.lip.pt/ulysses/Ulhistos_manual.pdf⟩ (accessed 2012).
[35] International Commission on Radiation Units and Measurements, ICRU Report 49, Stopping Powers and Ranges for Protons and Alpha Particles, 1993.
[36] PSTAR and ASTAR Databases for Protons and Helium Ions, ⟨http://physics.nist.gov/PhysRefData/Star/Text/programs.html⟩ (accessed 2012).
[37] X-Ray Mass Attenuation Coefficients, ⟨http://physics.nist.gov/PhysRefData/XrayMassCoef/tab1.html⟩ (accessed 2012).
[38] F.H. Attix, Introduction to Radiological Physics and Radiation Dosimetry, John Wiley & Sons, New York, 2008.
[39] M.J. Geary, K.M.M. Haque, NIM 137 (1976) 151.
[40] Atomic weights of the elements, IUPAC Technical Report, 2009, ⟨http://www.chem.qmul.ac.uk/iupac/AtWt/index.html⟩ (accessed 2012).
[41] M.E. Wieser, T.B. Coplen, Pure Appl. Chem. 83 (2) (2011) 359 http://dx.doi.org/10.1351/PAC-REP-10-09-14.